Taylor & Francis
Taylor & Francis Group

Infiltration of liquid metals in a nanoporous carbon

A. HAN, V. K. PUNYAMURTULA and Y. QIAO*

Department of Structural Engineering,
University of California – San Diego, La Jolla, CA 92093-0085, USA

Gallium and mercury are employed as liquid phases in a nanoporous carbon-based energy absorption system. Owing to the large surface tensions, the nanopore surface is non-wettable. Pressure-induced infiltration is observed and defiltration is difficult. The energy absorption efficiency is much higher than that of previously investigated nanoporous silica-based systems. The nominal solid–liquid interfacial tension is dependent on the nanopore size.

1. Introduction

Understanding the behaviour of liquids confined in nanoporous materials is immensely important to a variety of engineering applications, such as catalysis, mixture separation, absorption and adsorption [1–3]. When a large pore surface is exposed to functionally active agents, usually a liquid with or without suspended nanoparticles or macromolecules, beneficial chemical reactions or physical changes can be greatly amplified [4–6].

Recently, this concept has been extended to the area of mechanical engineering. For example, if a nanoporous material is surface-treated so that the nanopore walls are hydrophobic, spontaneous soaking can be prevented when it is immersed in water [7]. The control of degree of hydrophobicity may be achieved via surface group decoration [8] or network modification [9]. Under this condition, as a high external pressure is applied quasi-hydrostatically on the bulk water phase, water molecules can be forced to infiltrate into the nanopores. Since the liquid infiltration and defiltration process can be quite hysteretic, a large amount of external work is converted to solid–liquid interfacial tension over the large nanopore surface and cannot be released as the external load is removed. In other words, the nanoporous material functionalized (NMF) liquid is highly energy absorbing and this phenomenon can be employed for developing high-performance protective or damping devices. For another example, in certain types of nanoporous materials, as the liquid composition is appropriately adjusted, the confined liquid can defiltrate out of the nanopores quite smoothly as the pressure is lowered [10–12]. Such a system becomes a liquid spring, which may be applied for energy storage and active control.

---

*Corresponding author. Email: yqiao@ucsd.edu

In either case, the profile of sorption isotherm is dominant to the system performance. For the energy absorption system, the infiltration pressure, p_{in}, which is affected by the nanopore size and the solid–liquid interfacial tension, and the infiltration volume, V_{in}, which can be regarded as the volume of accessible nanopores, determine the energy absorption efficiency. Intensive studies have been conducted to develop NMF liquids of higher p_{in} and larger V_{in}. One promising way is to use nanoporous carbons. Compared with other nanoporous materials, such as alumina, silica gel, and zeolites and zeolite-like materials, nanoporous carbons have relatively small nanopore sizes and relatively large specific pore volumes. They are also much more cost-efficient, which is critical to large-scale engineering applications, such as liquid foundations, protection layers for highway bridges and buildings, etc. However, although at macroscopic length scale it was reported that a carbon material may be hydrophobic [13, 14], in a nano-environment, pressure-induced wetting can be difficult [15]. For instance, in a SEM study, Rossi *et al.* [16] argued that carbon nanotubes were wettable in water, which was in agreement with the conclusion of Dujardin *et al.* [17] that carbon nanotubes can be wetted by liquids with surface tensions smaller than 130–170 mJ/m^2. To utilize nanoporous carbons for energy absorption, liquid phases other than aqueous solutions need to be investigated.

In addition to p_{in} and V_{in}, which reflect the overall energy absorption efficiency, the profile of sorption isotherm, which determines the energy absorption process, is also important to system design and materials selection. If the profile of sorption isotherm is relatively steep, the liquid infiltration is less sensitive to external loading, and the system is more controllable while the working pressure range is broad. If the profile is relatively flat, the working pressure is confined in a narrow range while the system deformation can be somewhat unstable. When the pore size is larger than 100 nm, the liquid infiltration process can be discussed in the framework of conventional porosimetry analysis [18]; that is, the profile is determined by the pore size distribution. For nanopores, studies are still scarce.

In this article, we report the experimental results of infiltration of gallium and mercury in a nanoporous carbon. It is shown that, by using liquid metals, high-performance energy absorption systems can be developed. The testing data indicate that the profile of the sorption isotherm is dependent not only on the nanopore size distribution but also on the properties of the liquid phase.

2. Experimental

The nanoporous carbon under investigation was in powder form, provided by J. K. Baker, Inc. The average particle size was 50–80 μm. To increase the surface tension, the carbon was immersed in 40 ml of a 2.5% dry toluene solution of chlorotrimethylsilane and sealed in a flask that was protected from moisture by a drying tube. The temperature was maintained at 90°C for 12 h as the mixture was stirred by a magnetic stirrer, after which the carbon particles was collected by a filter, washed by dry toluene and warm water alternatively, and finally degassed at 100°C

in a vacuum oven for 0.5 h. During this process, the hydroxyl groups at nanopore surfaces were deactivated by $OSi(CH_3)_3$ groups [19].

The surface modified nanoporous carbon was mixed with poly(vinyidene) fluoride (PVF), with a carbon to PVF ratio of 5.7 in weight. The mixture was compressed by a type 5569 Instron machine under 20 MPa for 5 min at room temperature, forming thin disks of diameter 6.3 mm. The nanoporous structure was then analyzed by a Micromeritric Tristar 3000 analyzer with nitrogen at 77 K. Two loading tubes were used. One was the control sample, containing no solid materials; the other contained a carbon disk with a mass of 0.14 g. As a pressure was applied on the tubes, the mass difference between them, which reflected the amount of gas molecules absorbed at nanopore walls, was measured. The mass of infiltrated gas was a function of the external pressure, the nanopore size, as well as the specific nanopore surface area, from which the nanopore size distribution could be calculated. This procedure has been discussed in detail in [20].

The infiltration experiment was performed using mercury (Hg) and gallium (Ga). The sample was produced by sealing about 1200 mm^3 of liquid metal and a carbon disk in a steel cylinder by a piston. The mass of the carbon disk was 0.3 g. The cylinder and the piston were made of a high-carbon steel and air-cooled so as to increase the hardness. A reinforced O-ring couple was employed as the gasket. The Hg-based system was tested at room temperature and the Ga-based system at 40°C, with the temperature being controlled by a water bath. Using a type 5569 Instron machine, the piston was compressed in the cylinder quasi-statically at a constant rate of 0.5 mm/min. As the inner pressure reached 300–350 MPa, the crosshead was moved back. The loading–unloading process was repeated four times for each sample. The measured sorption isotherm curves are shown in figures 1 and 2. The sorption isotherm curves at the 3rd and the 4th loadings are not shown since they are similar to that at the 2nd loading.
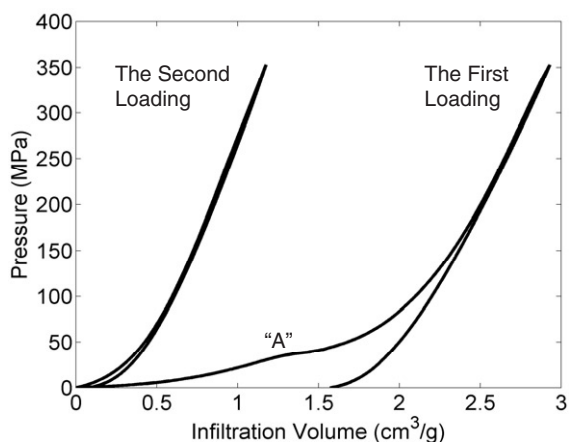
Figure 1.   Typical sorption isotherm curves of the gallium-based system.
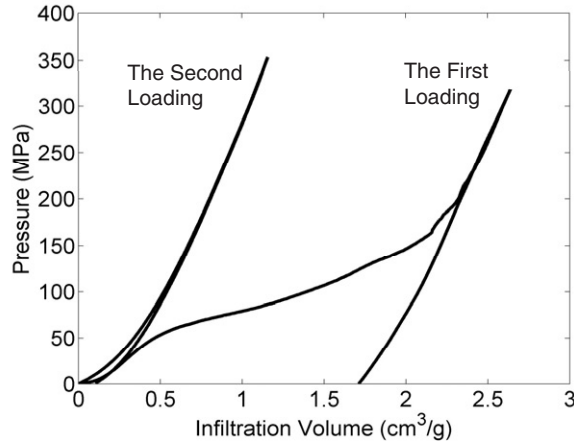
Figure 2.   Typical sorption isotherm curves of the mercury-based system.

3. Results and discussion

The melting point of gallium is 29.8°C [21] and, therefore, at the testing temperature it is in the liquid phase. If no external pressure is applied, at rest the system volume does not vary spontaneously, indicating that the nanopore surface is non-wettable. As the quasi-hydrostatic pressure increases, the infiltration volume becomes larger. The slope is quite small when the pressure is low. As a first-order approximation, the pressure can be related to the nanopore size through the classic Young's equation $p = 4\gamma/d$ [22], where γ is the interface tension, i.e. the capillary energy barrier that the liquid must overcome to enter a lyophobic channel, and d is the channel diameter. It can be seen that the required infiltration pressure, p, decreases as the pore size, d, increases. If the nanopore size distribution is perfectly uniform, as the infiltration rate is sufficiently low, the pressure should not increase with the infiltration depth, and thus the sorption isotherm curve tends to be flat. In reality, the nanopore size varies in a broad range owing to the imperfect structure of graphene layers, resulting in the profile of an infiltration plateau. If the specific volume of the largest nanopores is relatively high, infiltration of liquid phase begins at a relatively low pressure. In fact, if the pore size is beyond the nm level, infiltration can be triggered at a pressure smaller than 1 MPa, within the resolution of the testing machine. As the pore size becomes even larger, the pressure dependence of infiltration is further lowered and, eventually, infiltration can be spontaneous even with a hydrophobic pore surface, primarily due to the unstable free liquid surface. According to Young's equation, $r = 2\gamma/p$., where $r = d/2$ is the effective nanopore radius. The relative volume density of nanopores of radius r can be calculated as $c = \mathrm{d}V_\mathrm{p}/\mathrm{d}r$, where V_p is the volume of nanopores larger than r. If the slope of infiltration plateau is small, the nanopore size distribution tends to be broad; otherwise the nanopore size distributes in a narrow range.

From figure 1, it can be seen that at the low-pressure range, the slope of sorption isotherm is quite small, indicating that the c–r curve has a flat tail at the
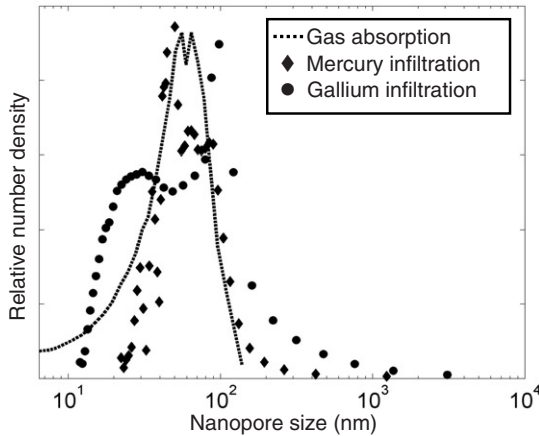
Figure 3. Comparison of nanopore size distribution curves obtained using different methods.

large nanopore size end. As the pressure increases, the slope becomes larger; that is, the nanopore size distribution approaches a peak. As the pressure reaches about 30 MPa, at point 'A', the slope decreases considerably, forming the second plateau in the pressure range of 30–50 MPa, which suggests that, at the intermediate nanopore size range, the variation of c is less pronounced. In the high-pressure range, the sorption isotherm curve is steep, which is attributed to the rapid change in volume fraction of relatively small nanopores. Finally, as p exceeds 170 MPa, the system becomes nearly incompressible, suggesting that the nanopores are filled. The calculated nanopore size distribution curve is shown in figure 3. If the value of γ associated with gallium infiltration is set to 165 mJ/m^2, the average nanopore size is close to the result of gas absorption analysis, which is shown by the dashed line. The largest nanopore size is at the μm level, corresponding to the low-pressure plateau in sorption isotherm. The smallest nanopore size calculated from the gallium infiltration data is smaller than that of the gas absorption analysis, probably because the motion of gallium molecules is more difficult than the diffusion of nitrogen molecules, especially when the nanopore size is comparable with or even smaller than the thickness of the solid–liquid interfacial layer.

After the infiltration is completed, as the pressure returns to zero, almost no gallium defiltration takes place, i.e. the state of gallium is metastable inside the nominally energetically unfavourable nanopores. Since the nanoporous carbon disk is no longer empty, when the pressure is reapplied, no sorption can be observed and the pressure–volume curve is nearly a straight line. As the sorption isotherm is hysteretic at the first loading, the external work is effectively dissipated. The energy absorption efficiency, which is the area enclosed by the loading–unloading cycle, is about 70 J/g, much higher than that of nanoporous-silica functionalized liquids [23]. As the temperature is reduced back to room temperature, the gallium inside the nanopores should be solidified and, consequently, a three-dimensional gallium nanonetwork is produced. This technique may be extended to other metals as the testing temperature is increased to above their melting points. Note that local

collapse of the nanoporous structure may take place owing to the large volume change.

When the liquid phase is mercury, the sorption isotherm curve changes significantly, as shown in figure 2. Compared with the gallium-based system, mercury infiltration at low pressure is much less evident, i.e. the critical pressure of infiltration increases. As the pressure is about 40 MPa, the sorption isotherm curve becomes flat and a wide infiltration plateau is formed until the nanopores are filled. Similar to the gallium-based system, unloading cannot trigger defiltration and at the second loading no infiltration can occur. The energy absorption efficiency in the first infiltration cycle is 145 J/g, much higher than the gallium system. If the effective excess solid–liquid interfacial tension is taken as 320 mJ/m^2, the nanopore size distribution is quite close to the gas absorption analysis result. Even the bimodal distribution around 60 nm is somewhat similar. In the large pore size range, the gas absorption analysis fails to give the value of c since the saturation time is longer than the testing time, while the smallest nanopores are not captured by the liquid metal infiltration tests. The viscosity of mercury and liquid gallium are 1.6 and 1.4 g/m/s, respectively. Although in a nanopore, on account of the large surface to volume ratio and the non-wettability of the solid surface, the effective viscosity may be lowered, these values are still much larger than the effective viscosity of nitrogen gas. Hence, the infiltration in nanopores smaller than a few nm might not be triggered in the pressure range of the current study.

Note that the effective excess solid–liquid interfacial tensions of mercury and gallium are determined merely for data-fitting purpose. The surface tension of mercury is about 480 mJ/m^2 and that of gallium is around 720 mJ/m^2 [21]. According to conventional surface theory [24], the carbon–mercury interfacial tension should be smaller. The nominal pore-size distribution obtained from the gallium infiltration experiment is broader than that obtained from the mercury infiltration experiment. Moreover, a comparison of figures 1 and 2 shows that infiltration volume of gallium is larger even though the nanoporous structure of the carbon should be the same. All these phenomena suggest that the effective solid–liquid interfacial tension in a nano-environment is size-dependent. The degree of size dependence is related to liquid properties. As the effective solid–gallium interfacial tension is smaller, the liquid phase can enter smaller nanopores. Hence, the infiltration pressure is lower and the measured infiltration volume is larger. The reason for the size dependence of γ is still under investigation; it is probably associated with the variation in molecular structure of the confined liquid as well as pressure-aided surface diffusion.

4. Conclusions

It has been validated that infiltration of liquid metals in a nanoporous carbon can be induced by external pressure. The infiltration of gallium is easier than that of mercury. The energy absorption efficiency associated with the liquid-metal infiltration is much higher than that of previously developed silica-based NMF liquids. The effective solid–liquid interfacial tension is dependent on the nanopore size.

Acknowledgement

References

[1] S. Polarz, B. Smarsly and J. Nanosci., Nanotechnol. **2** 581 (2002).
[2] N.Z. logar and V. Kaucic, Acta Chim. Slov. **53** 117 (2006).
[3] P.S. Grinchuk, Phys. Rev. E **66** 016124 (2002).
[4] A.B. Jarzebski, J. Mrowiec-Bialon and M. Kargol, Przemysl. Chem. **84** 410 (2005).
[5] J. Bisquert, D. Cahen, G. Hodes, *et al.*, J. Phys. Chem. B **108** 8106 (2004).
[6] A. Janes, H. Kurig and E. Lust, Carbon **45** 1226 (2007).
[7] X. Kong and Y. Qiao, Phil. Mag. Lett. **85** 331 (2005).
[8] A. Han and Y. Qiao, Chem. Lett. **36** 882 (2007).
[9] D. Dubbeldam and R.Q. Snurr, Mol. Simul. **33** 305 (2007).
[10] M. Soulard, J. Patarin, V. Eroshenko, *et al.*, Stud. Surf. Sci. Catal. **154** 1830 (2004).
[11] A. Laouir, L. Luo, D. Tondeur, *et al.*, AIChE J. **49** 764 (2003).
[12] A. Han and Y. Qiao, Phil. Mag. Lett. **87** 25 (2007).
[13] R.D. Narhe and D.A. Beysens, Langmuir **23** 6486 (2007).
[14] X.L. Xie, Y.W. Mai and X.P. Zhou, Mater. Sci. Eng. R **49** 89 (2005).
[15] V.K. Punyamurtula, A. Han and Y. Qiao, Adv. Eng. Mater. **9** 209 (2007).
[16] E. Dujardin, T.W. Ebbesen, A. Krishnan, *et al.*, Adv. Mater. **10** 1472 (1998).
[17] M.P. Rossi, H. Ye, Y. Gogtsi, *et al.*, Nano Lett. **4** 989 (2004).
[18] G.T. Shaw, *Porosimetry by Mercury Injection* (Department of Mines & Technical. Surveys, Mines Branch, Ottawa, Canada, 1963).
[19] M.H. Lim and A. Stein, Chem. Mater. **11** 3285 (1999).
[20] J. Keller and R. Staudt, *Gas Adsorption Equilibria: Experimental Methods and Adsorptive Isotherms* (Springer, Berlin, 2004).
[21] J.R. Davis, *Metals Handbook* (ASM International, Materials Park, OH, 1999).
[22] F.M. White, *Fluid Mechanics* (McGraw-Hill, New York, 2006).
[23] F.B. Surani, A. Han and Y. Qiao, J. Mater. Res. **21,** 2389 (2006).
[24] J.M. Howe, *Interfaces in Materials* (Wiley-Interscience, New York, 1997).